Published in final edited form as:
Anal Bioanal Chem. 2013 April ; 405(11): 3831–3838. doi:10.1007/s00216-012-6656-5.

A microfluidic electrochemiluminescent device for detecting cancer biomarker proteins

Naimish P. Sardesai[1], **Karteek Kadimisetty**[1], **Ronaldo Faria**[1,2], and **James F. Rusling**[1,3,4,*]

[1] Department of Chemistry, University of Connecticut, Storrs, CT 06269 USA

[2] Departamento de Química, Universidade Federal de São Carlos, SP, Brazil

[3]Department of Cell Biology, University of Connecticut Health Center, Farmington, CT 06032 USA

[4] Institute of Materials Science, University of Connecticut, Storrs, Connecticut 06269, USA

Abstract

We describe an electrochemiluminescence (ECL) immunoarray incorporated into a prototype microfluidic device for highly sensitive protein detection, and apply this system to accurate, sensitive measurements of prostate specific antigen (PSA) and interleukin-6 (IL-6) in serum. The microfluidic system employed three molded polydimethylsiloxane (PDMS) channels on a conductive pyrolytic graphite chip (PG) (2.5 × 2.5 cm) inserted into a machined chamber and interfaced with a pump, switching valve and sample injector. Each of the three PDMS channels encompasses three 3 μL analytical wells. Capture-antibody-decorated single-wall carbon nanotube (SWCNT) forests are fabricated in the bottom of the wells. The antigen is captured by these antibodies on the well bottoms. Then a RuBPY-silica-secondary antibody (Ab_2) label is injected to bind to antigen on the array, followed by injection of sacrificial reductant tripropylamine (TPrA) to produce ECL. For detection, the chip is placed into an open-top ECL measuring cell, and the channels are in contact with electrolyte in the chamber. Potential applied at 0.95 V vs. SCE oxidizes TPrA to produce ECL by redox cycling the RuBPY species in the particles, and ECL light is measured by a CCD camera. This approach achieved ultralow detection limits (DL) of 100 fg mL^{-1} for PSA (9 zeptomol) and 10 fg mL^{-1} (1 zeptomol) for IL-6 in calf serum, a 10-25 fold improvement of a similar non-microfluidic array. PSA and IL-6 in synthetic cancer patient serum samples were detected in 1.1 h and results correlated well with single-protein ELISAs.

Keywords

Microfluidics; Electrochemiluminescence; Immunoarray; Single-wall carbon nanotube forest; RuBPY-silica nanoparticles

Introduction

Rapid, automated multi-protein detection with moderate to high throughput is increasingly needed for clinical diagnostics using serum or tissue biomarker measurements [1-6]. Microfluidic devices can provide miniaturization, automation and parallelization of bioanalytical processes amenable to meeting such needs [7-8]. This paper describes a novel, sensitive microfluidic system designed to detect two proteins that is expandable to multiplexed determinations.

*Corresponding Author Tel.: +1 860 486 4909. Fax: +1 860 486 2981. james.rusling@uconn.edu..

Measurements of biomarker proteins hold enormous potential for early cancer detection and personalized therapy [1, 4-6]. Detecting elevated levels of *multiple* proteins in serum for a given cancer is necessary for high diagnostic accuracy. Multiple protein measurements involving microfluidics promises low cost, high sensitivity and accuracy, and possible point-of-care (POC) use to facilitate on-the-spot diagnosis and minimize patient stress [9-13].

Conventional methods for protein detection include enzyme-linked immunosorbent assay (ELISA) [1,6, 14], bead-based optical or electrochemiluminescent (ECL) methods [6], electrophoretic immunoassay [15] and mass spectrometry-based proteomics [16,17]. ELISA has long served as the gold standard for clinical protein assays [14], but is limited for multiplexing, by analysis time, and by sample volume required. LC/MS is an advanced tool for biomarker discovery, but is presently too complex and costly for routine diagnostics [17, 18]. Alternatively, selective and sensitive antibody microarrays of various kinds hold significant promise, as yet undelivered, for future automated protein measurements [1,6]

Heinemann et al. were among the first to develop microfluidic electrochemical immunoassays for proteins [19]. Subsequent microfluidic immunoassays have employed fluorescence [20,21], electrochemistry [22-27], surface plasmon resonance (SPR) [28,29], paper devices [30-33] and integrated chips [34-36]. Microfluidic systems directed toward POC detection of nucleic acids and proteins have been explored [10,13]. To date, however, few approaches have achieved the combination of low cost, speed, high sensitivity, accuracy, and technical simplicity suitable for clinical applications or POC.

We recently developed an amperometric microfluidic immunoarray for simultaneous detection of biomarker proteins using off-line capture on massively labeled magnetic particles [24]. This strategy gave detection limits (DL) into the 5-50 fg mL^{-1} range for oral cancer biomarker proteins in 50 min. assays of diluted serum [37]. We also developed gold arrays by processing gold CDs and fabricating microwells around the sensor electrodes and combined them with a multilabel strategy to achieve a 10 fg mL^{-1} DL for interleukin IL-6 [38].

Electrochemiluminescence (ECL), an electrode-driven luminescent process, is a sensitive alternative to amperometric detection that can employ very simple array chips. Light emission is initiated utilizing electrochemistry at the sensor surface [39-42]. Using the complex $Ru(bpy)_3^{2+}$ (RuBPY), ECL light is produced in a multistep catalytic redox process featuring sacrificial reductant tripropylamine (TprA) to yield photo-excited $[Ru(bpy)_3^{2+}]^*$ that emits at 610 nm. This approach has been used in various types of sandwich immunoassays, including commercial magnetic bead-based protein detection [39,41-44]. However, commercial automated ECL bead technology is relatively expensive and usually requires significant technical expertise and maintenance [6,45].

We have combined single-wall carbon nanotube (SWCNT) forest sensors [46] with RuBPY-silica nanoparticle labels for accurate, sensitive detection of PSA in cancer patient serum [47]. RuBPY-silica nanoparticles provide amplification by incorporating thousands of RuBPY ions. We recently integrated this approach into an manual array format featuring hydrophobic wells fabricated around analytical spots on a conductive pyrolytic graphite (PG) chip [48]. These earlier non-microfluidic arrays provided simultaneous detection of prostate specific antigen (PSA) with DL 1 pg $mL^{-1}$and IL-6 at 0.25 pg mL^{-1} in serum. This approach has an advantage that multi-electrode chip is not needed as in amperometric detection. The manual array comprises of a PG chip as the working electrode with spatially separated wells in a single symmetric electrochemical cell. The 10 μL analytical wells featured SWCNT forests at the bottom decorated with capture antibodies to enable sandwich immunoassays. After protein analyte was captured from the sample onto the chip, the

RuBPY-silica label decorated with a second antibody was added, potential applied, and ECL light detected with a charge-coupled device (CCD) camera.

In the current paper, we incorporate for the first time a carbon nanotube-based microwell ECL immunoarray into a microfluidic system utilizing RuBPY-silica particles (Fig. 1). The device features three 90 μL rectangular polydimethylsiloxane (PDMS) channels on a PG chip supported by a hard, flat, machined poly(methylmethacrylate) (PMMA) plate. Fabrication involves only conventional machining. The top PMMA plate is equipped with symmetric Ag/AgCl reference and Pt counter electrode wires that run along the tops of the channels to form symmetric electrochemical cells. Analytical spots are positioned on the PG at the channel bottom. The assembled microfluidic device is connected to a pump, injector and a 3-way valve that guides solutions to the desired channel. The immunoarray provided simultaneous detection of biomarker proteins PSA and IL-6 in serum, giving high sensitivity and DLs in the low fg mL^{-1} range (zemptomol range), representing 10-25 fold improvement over our previous non-microfluidic ECL array. Good correlations with single protein ELISAs were obtained on pooled prostate cancer patient serum samples.

Materials and methods

Chemicals and immunochemicals

Lyophilized 99% bovine serum albumin (BSA), Tween-20, Tris(2,2-bipyridyl)dichlororuthenium-(II) hexahydrate, poly(diallydimethylammonium chloride) (PDDA), polyacrylic acid (PAA), and tripropylamine (TPrA), 1-(3-(dimethylamino)-propyl)-3- ethylcarbodiimide hydrochloride (EDC) and N-hydroxysulfosuccinimide (NHSS) were from Sigma/Aldrich. Single-walled carbon nanotubes (HiPco) were from Carbon Nanotechnologies, Inc. Monoclonal (mouse) primary antihuman prostate specific antigen (PSA) antibody (CHYH1), tracer secondary anti-PSA antibody, and PSA standards were from Anogen/Yes Biotech Lab, Ltd. Monoclonal antihuman interleukin-6 (IL-6) antibody (clone no. 6708), biotinylated antihuman IL-6 antibody, recombinant human IL-6 (carrier-free) were from R&D Systems, Inc.. Human serum samples were purchased from Capital Biosciences. Pyrolytic graphite block (2.5 cm × 2.5 cm) was obtained from Advanced Ceramics. RuBPY-silica particles were prepared as described previously [47, 48]. The average particle diameter from TEM was 92 ± 8 nm (see Fig. S1, Electronic Supplementary Material). The ECL labels were prepared by coating RuBPY-silica particles with poly(acrylic acid), and then attaching the particles to secondary antibodies to PSA (PSA-Ab_2) and IL-6 (IL-6-Ab_2) by amidization with EDC/NHSS. Fluorescence spectra of the antibody and RuBPY were used to estimate concentrations of secondary antibodies and [[Ru-$(bpy)_3]^{2+}$] in RuBPY-silica particles (Fig. S2 and S3, Electronic Supplementary Material). From these studies, Ab_2/ RuBPY-silica particle ratio was estimated at 26: 1 and there were 1.6×10^6 RuBPY per silica particles. These particles provided 3-fold increase in RuBPY concentration compared to the particles used with a previous non-microfluidic array [48] due to a 4-fold increase in RuBPY concentration in the solution used to synthesize the RuBPY-silica nanoparticles (see SI).

Solutions

Immunoreagents were dissolved in pH 7.2 phosphate buffer saline (PBS) (0.01 M phosphate, 0.14 M NaCl, 2.7 mM KCl), unless otherwise noted. Co-reactant solution was 100 mM tripropylamine (TPrA) with 0.05% Tween 20 (T-20) and 0.05% Triton-X in 0.2 M phosphate buffer (pH: 7.5).

Instrumentation

We designed a prototype ECL microfluidic device utilizing a similar approach used in our earlier amperometric microfluidic device [24]. A soft PDMS slab was molded on an aluminum template to have three rectangular channels. This PDMS slab was placed on top of a PG block equipped with rectangular (1 mm × 2 mm) analytical wells surrounded by ~hydrophobic polymer borders drawn with a Pap pen (Sigma Adrich), using a template as described previously [48]. Each well had a volume of 3.0 ± 0.2 μL. SWCNT forests were assembled in the bottoms of the microwells and primary antibodies attached to their carboxylated ends [48] (Fig. 1, Fig. S4a and S4b, Electronic Supplementary Material). This assembly was sandwiched between two hard flat PMMA plates, and bolted together tightly to provide three microfluidic channels (Fig. 1, and Fig. S4c, Electronic Supplementary Material). Each microfluidic channel was 2 mm wide, 2.5 cm long, and had a volume of 92 μL. This device housed Ag/AgCl reference and Pt counter wires placed symmetrically in each channel [24]. This assembly was further modified because PMMA is not optically transparent and can partially block light. Therefore sections of PMMA right above the analytical spots were removed and replaced with optical glass (see Fig. S4c, Electronic Supplementary Material). A syringe pump (Harvard, 55-3333, Upchurch Scientific) was connected to an injector valve (Rheodyne, 9725i, Upchurch Scientific), and a switch valve (Rheodyne, 9060, Upchurch Scientific) in series. The switch valve was connected to the inlets of the three channels (see Fig. S4d, Electronic Supplementary Material). Reagents were injected into the sample loop through the injector valve and guided by the switch valve to the desired channel. The device was housed in dark box, a CH Instruments model 1232 electrochemical analyzer was used to apply voltage, and a CCD camera was used to measure the ECL light [48]. The CCD Camera (Syngene, UK) had a resolution of 5 mega pixel, dynamic range of 4.8 OD and Ultra Peltier cooling with forced air for extra long exposures.

Microfluidic immunoassay protocol

Cognate capture antibodies (Ab_1) for PSA and IL-6 were attached to carboxylic groups of SWCNT forests in the wells by EDC-NHS amidization [48]. Before each assay, a solution of 2% BSA in PBS containing 0.05% T-20 was passed into the microfluidic channels to block non-specific binding on analytical spots and channel surfaces. Flow was stopped and the BSA solution was left in the system for 30 min, followed by washing with PBS-T20 and PBS. Then, PSA or IL-6 standard or sample solution was injected to fill the 100 μL sample loop. The switch valve was used to guide the solution in one of the three channels at 100 μL min^{-1} and the flow was stopped. This procedure was repeated to fill all the three channels. After every antigen injection the sample loop was washed with PBS. Antigen was incubated for 30 min. followed by washing with PBS and PBS tween-20. This ECL label particle dispersion was then injected to fill all three channels, and incubation was allowed for 15 min. followed by washing step with PBS-T20 and PBS. The 100 μL ECL label features RuBPY-silica-nanoparticles, containing 0.15 mg mL^{-1} $[[Ru\text{-}(bpy)_3]^{2+}]$, attached to mixture of PSA-Ab_2 and IL-6-Ab_2 (50.4 ng mL^{-1}) (see SI). Then 100 mM tripropylamine was injected into each channel, a potential of 0.95 V versus Ag/AgCl was applied, and ECL was collected with the CCD camera for 400 s.

Results

Reproducibility and Calibrations

Spot-to-spot reproducibility of ECL responses in the three microfluidic channels was first characterized using immunoassays of PSA and IL-6. With PSA capture antibodies attached to the SWCNT forests, BSA solution was injected in the channels to block non-specific binding (NSB), incubated for 30 min., then washed out with PBS-T20 and PBS. Protein standards were then injected into the channels and incubated 30 min. with the flow stopped.

Then, a dispersion of the RuBPY-silica-Ab_2 label was injected and flow continued until it completely filled the channels, as evidenced by the red-brown color of the particles. Flow was stopped and 15 min incubation was allowed for the antibodies in the analytical wells to capture the particles. This step was followed by injection of TPrA solution containing surfactants into the system. Then, a potential at 0.95 V versus Ag/AgCl was applied to oxidize TPrA to initiate the ECL response [47]. ECL was then measured by using a CCD camera and integrating signal over time.

Results showed that the spots in the three channels for the zero PSA controls gave relative ECL intensities within ± 5% (see Fig. 2a). Immunoassay results for PSA and IL-6 at selected concentrations also showed good reproducibility (see Fig. 2b and 2c). Microfluidic ECL arrays gave reproducible signals for PSA (Fig. 2b), IL-6 and controls (see Fig. 2c) in calf serum. Relative ECL intensities for each antigen were reproducible in most cases to better than ±10% (see Fig. S5, Electronic Supplementary Material).

The PSA and IL-6 antibodies used in this work are minimally cross-reactive with non-cognate proteins under our assay conditions [48]. The protocol for determination of the two proteins in mixtures utilized label particles that featured secondary antibodies to both PSA and IL-6 conjugated to a single RuBPY-silica nanoparticle, and the RuBPY-silica particles were loaded with 3-fold more [$[Ru\text{-}(bpy)_3]^{2+}$] than used earlier [48] (see Electronic Supplementary Material).

CCD images for PSA and IL-6 mixtures on the same array are shown in Fig. 3 and Fig. S7, Electronic Supplementary Material. There was no significant difference between the ECL signals obtained using single or mixed antibodies attached to RuBPY-silica nanoparticles (see Fig. S8, Electronic Supplementary Material). For two protein detection, the microfluidic ECL arrays provided sensitivity at clinically relevant levels of PSA from 100 fg mL^{-1} to 10 ng mL^{-1} and IL-6 from 10 fg mL^{-1} to 1 ng mL^{-1} (see Fig. 4). The DL estimated as three times the standard deviation above the ECL signal for the antigen-free control were 100 fg mL^{-1} for (9 zeptomol) PSA and 10 fg mL^{-1} (1 zeptomol) for IL-6, and were similar to that for single biomarker detection (see Figs. 4 and Fig. S6, Electronic Supplementary Material). The sensitivities of 6.25×10^3 relative photon intensity-mL pg^{-1} for PSA and 6.8×10^4 relative photon intensity-mL pg^{-1} for IL-6 were obtained as slopes of the linear calibration graph in the lower range of antigen concentration (see Fig. S9, Electronic Supplementary Material, and Table 1).

Analysis of Serum Samples

The accuracy of microfluidic arrays was validated by determining PSA and IL-6 using human serum samples and was compared with single-protein ELISAs (see Figs. 5 and S10, Electronic Supplementary Material). Samples 1-5 represent pooled serum from prostate cancer patients, while sample 6 was obtained from cancer-free patients. Surprisingly, these commercial serum samples were very low in IL-6, and so were spiked with known concentrations of pure IL-6 protein to make 6 synthetic serum samples containing measureable quantities of PSA and IL-6. These were diluted 40-fold with calf serum to evaluate the performance of the device using synthetic mixtures containing PSA and IL-6 in a mixed full-serum medium. The samples were diluted to fall within the dynamic ranges of the calibration graphs. Assay results showed very similar levels of PSA and IL-6 by ECL immunoarray and single protein ELISA (Fig. 5); t-tests at the 95% confidence level confirmed no significant differences between the two methods (see Fig. S11 and Table S1, Electronic Supplementary Material). ECL array results gave very good linear correlation plots with ELISA for all samples with slopes close to 1.0, intercepts near zero, and correlation coefficients of 0.998 (see Fig. S11 and Table S1, Electronic Supplementary

Material). In addition, a very good correspondence was obtained between the amount of IL-6 spiked and the amount found by the immunoarray (Fig. 5b).

Discussion

Results described above show clearly that the microfluidic arrays described here utilizing multilabel ECL particles and SWCNT forests in 10 μL microwells are capable of simultaneous ultrasensitive detection of two proteins in serum at levels down into 10-100 fg mL^{-1} range (Figs. 3-5). In addition, the SWCNT forest assembly is easy to prepare and cost effective (~3 cents/per array). The geometry of such assembly provides high conductive surface for biosensing. The main advantage of this prototype device is that it offers a rapid, simple, inexpensive [24] way to simultaneously detect two biomarker proteins in serum in an assay time of 1.1 hr without using sophisticated microelectronics or lithographic fabrication. Moreover, the DLs for microfluidic ECL arrays are much better than the best values of about 1 pg mL^{-1} of commercial multiplexed bead-based ECL protein assays. Also, compared with our previously reported manually operated ECL protein arrays [48], these microfluidic ECL arrays provided 10-fold better DL for PSA, and 25-fold better for IL-6. A DL of 100 fg mL^{-1} (9 zeptomol) was obtained for PSA using microfluidic arrays compared to 1 pg mL^{-1} (90 zeptomol) using the non-microfluidic array, and DL of 10 fg mL^{-1} (1 zeptomol) for Il-6 using microfluidic arrays compared to 0.25 pg mL^{-1} (25 zeptomol) using manual arrays. Assay times were decreased to 1.1 hr using the microfluidic arrays from the 3 hrs required for the non-microfluidic arrays. Moreover, microfluidic arrays used only 3 μL of expensive immunoreagent solutions per microwell compared to manual arrays that used 5-10 μL of solution [48]. The 92 μL volume of the microfluidic channels is justified because of the high sensitivity of the microfluidic immunoarrays that allowed patient samples to be diluted 40 fold as opposed to 2-fold dilution in our non-microfluidic arrays. The microfluidic arrays required 2.5 μL of patient samples for triplicate analyses, whereas in non-microfluidic arrays, 2.5 μL of sample was used for a single analysis.

The higher efficiency of the microfluidic arrays is likely due to a number of factors. First, a larger surface area to volume ratio in the microchannels and the decrease in sample volume tend to increase antigen capture efficiency due to large number of capture antibodies present on the surface [49]. Second, the microchannels [49] facilitate mass transport that is not present in the manual protocols. This may enhance production and deprotonation of $TPrA\bullet^{+}$ necessary to give TPrA• to reduce $[Ru\text{-}(bpy)_3]^{2+}$ to $[Ru\text{-}(bpy)_3]^{+}$ [50], which combines with $[Ru\text{-}(bpy)_3]^{3+}$ to provide the ECL producing $*[Ru\text{-}(bpy)_3]^{2+}$. Third, higher sensitivity than the manual array is realized due to the use of RuBPY-silica particles loaded with ~1.6×10^6 $[[Ru(bpy)_3]^{2+}]$ per particle, which is 3-fold more compared to the particles previously reported manual ECL arrays [48] (see SI). Also, the Ab_2/RuBPY-Silica particle ratio was 26:1 which provides good capture efficiency. In addition, the SWCNT forest in the well bottoms provide a high area nanostructure surface that enables attachment of a high surface concentration of capture antibodies to provide an additional 3-10 fold signal enhancement compared to flat surfaces [47,51].

Semi-log calibration graphs for PSA and IL-6 were curved upward, reflecting better sensitivity at the higher concentrations. Though not linear, these calibration curves are quite suitable for practical analyses of biomedical samples in clinically relevant ranges. The assay results on synthetic serum samples by the microfluidic ECL array gave excellent correlations with standard ELISA assays for detection of both proteins (Figs. 5 and Fig. S11, Electronic Supplementary Material).

In summary, we have described here a microfluidic ECL immunosensor for two proteins, and demonstrated PSA and IL-6 detection in synthetic serum samples to show that sensitive

and accurate detection of at least two biomarkers in serum is possible. Detection limits for IL-6 and PSA on the microfluidic ECL arrays are significantly better than those for ELISA and for commercial bead-based protein assay systems. An improved version of this ECL microfluidic device is currently being equipped with micro-pumps to develop a miniaturized, automated, system to detect a larger number of biomarkers.

Supplementary Material

Refer to Web version on PubMed Central for supplementary material.

Acknowledgments

This work was supported by Grant No. EB014586 from the National Institute of Biomedical Imaging and Bioengineering (NIBIB), NIH. We also acknowledge FAPESP Proc. No. 11/02259-6 for financial support to Dr. R. C. Faria for a sabbatical visit.

References

1. Kingsmore SF. Multiplexed protein measurement: technologies and applications of protein and antibody arrays. Nat Rev Drug Discovery. 2006; 5:310–320.
2. Ferrari M. Cancer nanotechnology: opportunities and challenges. Nat Rev Cancer. 2005; 5:161–171. [PubMed: 15738981]
3. Wulfkuhle JD, Liotta LA, Petricoin EF. Proteomic applications for the early detection of cancer. Nat Rev Cancer. 2003; 3:267–275. [PubMed: 12671665]
4. Giljohann DA, Mirkin CA. Drivers of biodiagnostic development. Nature. 2009; 426:461–464. [PubMed: 19940916]
5. Ludwig JA, Weinstein JN. Biomarkers in cancer staging, prognosis and treatment selection. Nature Rev Cancer. 2005; 5:845–856. [PubMed: 16239904]
6. Rusling JF, Kumar CV, Patel V, Gutkind JS. Measurement of biomarker proteins for point-of-care early detection and monitoring of cancer. Analyst. 2010; 135:2496–2511. [PubMed: 20614087]
7. Zhang C, Xing D. Single-Molecule DNA Amplification and Analysis Using Microfluidics. Chem Rev. 2010; 110:4910–4947. [PubMed: 20394378]
8. Gupta K, Kim D, Ellison D, Smith C, Kundu A, Tuan J, Suhc K, Levchenko A. Lab-on a-chip devices as an emerging platform for stem cell biology. Lab Chip. 2010; 10:2019–2031. [PubMed: 20556297]
9. Gubala V, Harris LF, Ricco AJ, Tan MX, Williams DE. Point of care diagnostics: status and future. Anal Chem. 2012; 84:487–515. [PubMed: 22221172]
10. Choi S, Goryll M, Sin L, Wong PK, Chae J. Microfluidic-based biosensors toward point-of-care detection of nucleic acids and proteins. Microfluidics and Nanofluidics. 2011; 10:231–247.
11. Mohammed M, Desmulliez M. Lab-on-a-chip based immunosensor principles and technologies for the detection of cardiac biomarkers: a review. Lab Chip. 2011; 11:569–595. [PubMed: 21180774]
12. Pagaduan JV, Yang W, Woolley AT. Optimization of monolithic columns for microfluidic devices. Proc SPIE. 2011; 8031:80311V.
13. Ng A, Uddayasankar U, Wheeler AR. Immunoassays in microfluidic systems. Anal Bioanal Chem. 2010; 397:991–1007. [PubMed: 20422163]
14. Findlay JW, Smith WC, Lee JW, Nordblom GD, Das I, DeSilva BS, Khan MN, Bowsher RR. Validation of immunoassays for bioanalysis: a pharmaceutical industry perspective. J Pharm Biomed Anal. 2000; 21:1249–1273. [PubMed: 10708409]
15. Schmalzing D, Nashabeh W. Capillary elecúophoresis based immunoassays: A critical review. Electrophoresis. 1997; 18:2184–2193. [PubMed: 9456033]
16. Aebersold R, Mann M. Mass spectrometry-based proteomics. Nature. 2003; 422:198–207. [PubMed: 12634793]
17. Hawkridge AM, Muddiman DC. Mass spectrometry-based biomarker discovery: toward a global proteome index of individuality. Ann Rev Anal Chem. 2009; 2:265–277.

18. Hanash SM, Pitteri SJ, Faca VM. Mining the plasma proteome for cancer biomarkers. Nature. 2008; 452:571–579. [PubMed: 18385731]
19. Bange A, Halsall HB, Heinemann WR. Microfluidic immunosensor systems. Biosens Bioelectron. 2005; 20:2488–2503. [PubMed: 15854821]
20. Gervaisab L, Delamarche E. Toward one-step point-of-care immunodiagnostics using capillary-driven microfluidics and PDMS substrates. Lab Chip. 2009; 9:3330–3337. [PubMed: 19904397]
21. Garcia-Alonso J, et al. Micro-screening Toxicity System based on Living Magnetic Yeast and Gradient Chips. Anal. Bioanal. Chem. 2011; 400:1009–1013. [PubMed: 20924564]
22. Fosdick SF, Crooks JA, Chang BY, Crooks RM. Two-Dimensional Bipolar Electrochemistry. J Am Chem Soc. 2010; 132:9226–9227. [PubMed: 20557049]
23. Stern E, Vacic A, Rajan NK, Criscione JM, Park J, Ilic BR, Mooney DJ, Reed MA, Fahmy TM. Label-free biomarker detection from whole blood. Nat Nanotechnol. 2010; 5:138–42. [PubMed: 20010825]
24. Chikkaveeraiah BV, Mani V, Patel V, Gutkind JS, Rusling JF. Microfluidic electrochemical immunoarray for ultrasensitive detection of two cancer biomarker proteins in serum. Biosens Bioelectron. 2011; 26:4477–4483. [PubMed: 21632234]
25. Li Q, Tang D, Tang J, Su B, Chen G, Wei M. Magneto-controlled electrochemical immunosensor for direct detection of squamous cell carcinoma antigen by using serum as supporting electrolyte. Biosens Bioelectron. 2011; 27:153–159. [PubMed: 21782413]
26. Fragoso A, Latta D, Laboria N, Germar F, Hansen-Hagge T, Kemmner W, G€artner C, Klemm R, Dreseb K, O'Sullivan C. Integrated microfluidic platform for the electrochemical detection of breast cancer markers in patient serum samples. Lab Chip. 2011; 11:625–631. [PubMed: 21120243]
27. Kellner C, Botero ML, Latta D, Drese K, Fragoso A, O'Sullivan C. Automated microsystem for electrochemical detection of cancer markers. Electrophoresis. 2011; 32:926–930. [PubMed: 21394733]
28. Choi S, Chae C. A microfluidic biosensor based on competitive protein adsorption for thyroglobulin detection. Biosens Bioelectron. 2009; 25:118–123. [PubMed: 19577460]
29. Jeon S, Kim SU, Jeon W, Shin CB. Fabrication of Multicomponent Protein Microarrays with Microfluidic Devices of Poly(dimethylsiloxane). Macromolecular Research. 2009; 17:192–196.
30. a Cheng CM, Martinez AW, Gong J, Mace CR, Phillips ST, Carrilho EC, Mirica KA, Whitesides GM. Millimeter-Scale Contact Printing of Aqueous Solutions using a Stamp Made out of Paper and Tape. Lab on a Chip. 2010; 10:3201–3205. [PubMed: 20949218] b Martinez AW, Phillips ST, Butte MJ, Whitesides GM. Patterned paper as a platform for inexpensive, low-volume, portable bioassays. Angew Chem Int Ed. 2007; 46:1318–1320.c Sia SK, Linder V, Parviz B, Siegel A, Whitesides GM. An integrated approach to a portable and low-cost immunoassay for resource-poor settings. Angew Chem. 2004; 116:504–508.
31. Liu H, Crooks RM. A Paper-Based Electrochemical Sensing Platform with Integral Battery and Electrochromic Read-out. Anal Chem. 2012; 84:2528–2532. [PubMed: 22394093]
32. Ge L, Yan J, Song X, Yan M, Ge S, Yu J. Three-dimensional paper-based electrochemiluminescence immunodevice for multiplexed measurement of biomarkers and point-of-care testing. Biomaterials. 2012; 33:1024–1031. [PubMed: 22074665]
33. Delaney JL, Hogan CF, Tian J, Shen W. Electrogenerated chemiluminescence detection in paper-based microfluidic sensors. Anal Chem. 2011; 83:1300–1306. [PubMed: 21247195]
34. Pittet P, Lu G, Galvan J, Ferrigno R, Blum L, Leca-Bouvier B. PCB Technology-Based Electrochemiluminescence Microfluidic Device for Low-Cost Portable Analytical Systems. IEEE SENSORS JOURNAL. 2008; 8:565–571.
35. Pittet P, Lu G, Galvan J, Ferrigno R, Blum L, Leca-Bouvier B. PCB-based integration of electrochemiluminescence detection for microfluidic systems. Analyst. 2007; 132:409–411. [PubMed: 17471385]
36. Niskanen AJ, Ylinen-Hinkka T, Kulmala S, Franssila S. Integrated microelectrode hot electron electrochemiluminescent sensor for microfluidic applications. Sensors and Actuators B. 2011; 152:56–62.

37. Malhotra R, Patel V, Chikkaveeraiah BV, Munge BS, Cheong SC, Zain RB, Abraham MT, Dey DK, Gutkind JS, Rusling JF. Oral Cancer Detection in the Clinic Using an Ultrasensitive Microfluidic Array for a Panel of Biomarker Proteins. Anal Chem. 2012; 84:6249–6255. [PubMed: 22697359]
38. Tang CK, Vaze A, Rusling JF. Fabrication of immunosensor microwell arrays from gold compact discs for detection of cancer biomarker proteins. Lab Chip. 2011; 12:281–286. [PubMed: 22116194]
39. Debad, JB.; Glezer, EN.; Leland, JK.; Sigal, GB.; Wholstadter, J. Electrogenerated Chemiluminescence. Bard, AJ., editor. Marcel Dekker; 2011. p. 359-396.
40. Miao WJ. Electrogenerated Chemiluminescence and Its Biorelated Applications. Chem Rev. 2008; 108:2506–2553. [PubMed: 18505298]
41. Richter MM. Electrochemiluminescence (ECL). Chem Rev. 2004; 104:3003–3036. [PubMed: 15186186]
42. Forster RJ, Bertoncello P, Keyes TE. Electrogenerated Chemiluminescence. Annu Rev Anal Chem. 2009; 2:359–385.
43. http://rochediagnostics.ca/lab/solutions/e2010.php
44. http://www.meso-scale.com/CatalogSystemWeb/WebRoot/technology/ecl.htm
45. Healy DA, Hayes CJ, Leonard P, McKenna L, O'Kennedy R. Biosensor developments: application to prostate-specific antigen detection. Trends Biotechnol. 2007; 25:125–131. [PubMed: 17257699]
46. a Yu X, Munge B, Patel V, Jensen G, Bhirde A, Gong JD, Kim SN, Gillespie J, Gutkind JS, Papadimitrakopoulos F, Rusling JF. Carbon Nanotube Amplification Strategies for Highly Sensitive Immunodetection of Cancer Biomarkers. J Am Chem Soc. 2006; 128:11199–11205. [PubMed: 16925438] b Kim SN, Rusling JF, Papadimitrakopolous F. Carbon Nanotubes for Electronic and Electrochemical Detection of Biomolecules. Adv Mater. 2007; 19:3214–3228. [PubMed: 18846263] c Rusling, JF.; Yu, X.; Munge, BS.; Kim, SN.; Papadimitrakopoulos, F. Engineering the Bioelectronic Interface. Davis, J., editor. Royal Society of Chemistry; 2009. p. 94-118.
47. Sardesai NP, Pan S, Rusling JF. Electrochemiluminescent immunosensor for detection of protein cancer biomarkers using carbon nanotube forests and $[Ru\text{-}(bpy)_3]^{2+}$-doped silica nanoparticles. Chem Commun. 2009:4968–4970.
48. Sardesai NP, Barron J, Rusling JF. Carbon Nanotube Microwell Array for Sensitive Electrochemiluminescent Detection of Cancer Biomarker Proteins. Anal Chem. 2011; 83:6698–6703. [PubMed: 21728322]
49. Kai J, Puntambekar A, Santiago N, Lee SH, Sehy DW, Moore V, Han J, Ahn C. A novel microfluidic microplate as the next generation assay platform for enzyme linked immunoassays (ELISA). Lab on a Chip. 2012 Doi:10.1039/C2LC40585G.
50. Miao W, Choi JP, Bard AJ. Electrogenerated chemiluminescence 69: the tris(2,2′-bipyridine)ruthenium(II), $(Ru(bpy)_3^{2+})$/tri-n-propylamine (TPrA) system revisited-a new route involving $TPrA^{*+}$ cation radicals. J. Am. Chem. Soc. 2002; 124:14478. [PubMed: 12452725]
51. Malhotra R, Papadimitrakopoulos F, Rusling JF. Sequential Layer Analysis of Protein Immunosensors Based on Single Wall Carbon Nanotube Forests. Langmuir. 2010; 26:15050–15056. [PubMed: 20731335]

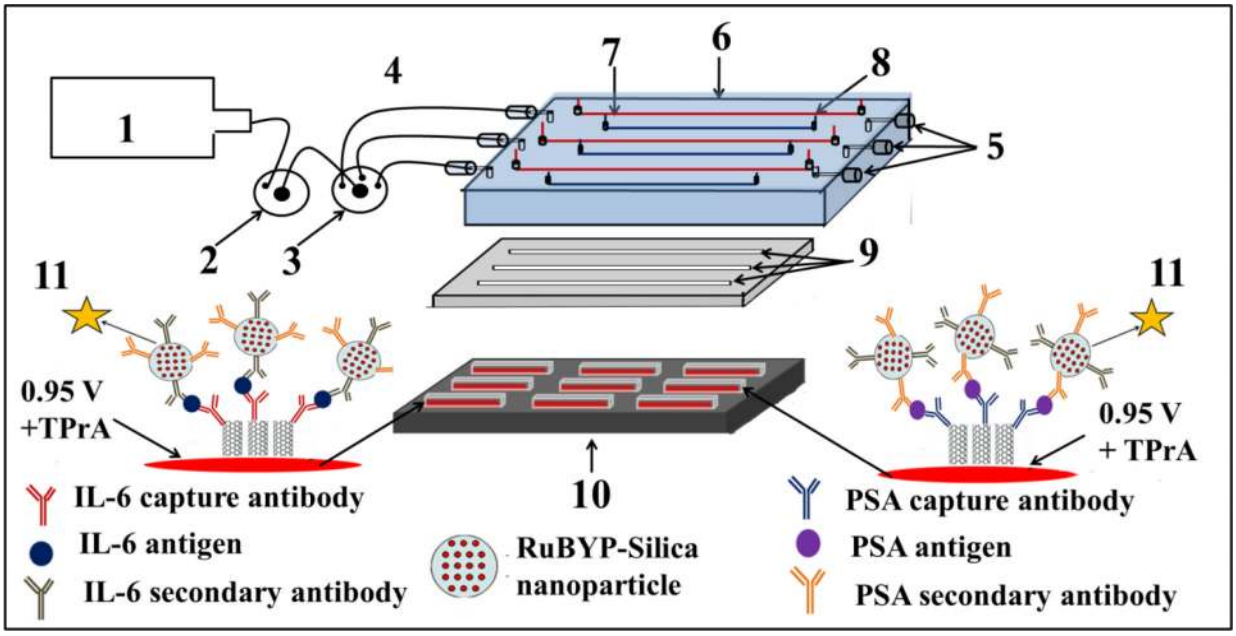

Fig. 1.

Design of microfluidic ECL array: 1) syringe pump 2) injector valve, 3) switch valve to guide the sample to the desired channel, 4) tubing for inlet, 5) outlet, 6) poly(methylmethacrylate) (PMMA) plate, 7) Pt counter wire, 8) Ag/AgCl reference wire (wires are on the underside of PMMA plate), 9) polydimethylsiloxane (PDMS) channels, 10) pyrolytic graphite chip (PG) (2.5 cm × 2.5 cm) (black), surrounded by hydrophobic polymer (white) to make microwells. Bottoms of microwells (red rectangles) contain primary antibody-decorated SWCNT forests, 11) ECL label containing RuBPY-silica nanoparticles with cognate secondary antibodies are injected to the capture protein analytes previously bound to cognate primary antibodies. ECL is detected with a CCD camera.

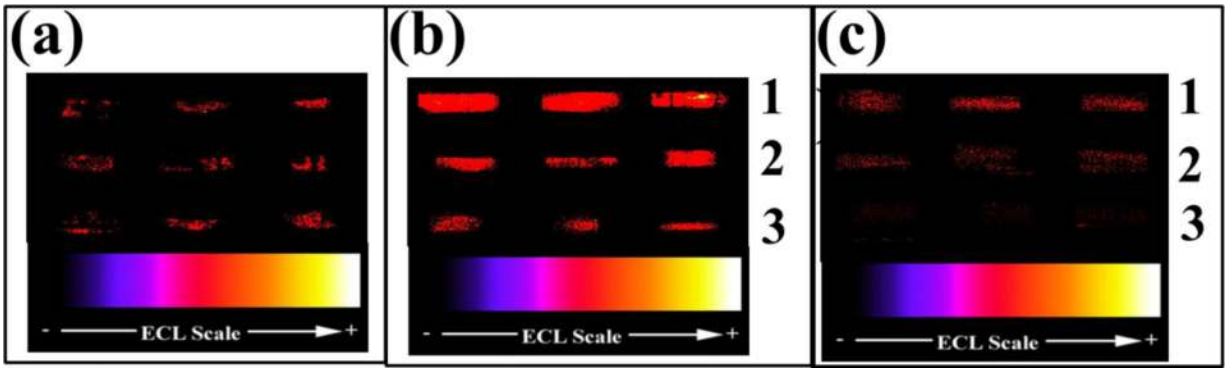

Fig. 2.

CCD images of microfluidic immunoarrays showing reproducibility for PSA and IL-6 alone in calf serum: (a) all spots for 0 PSA (control), (b) Lanes: **1**) 10 pg mL^{-1} PSA, **2**) 100 fg mL^{-1} PSA, and **3**) 0 PSA (control), (c) Lanes: **1**) 100 fg mL^{-1} IL-6, **2**) 10 fg mL^{-1} IL-6, and **3**) 0 IL-6 (control). ECL images obtained at 0.95 V vs. Ag/AgCl in the presence of 0.05% Tween 20 + 0.05% Triton-X 100 + 100 mM TPrA in 0.2 M phosphate buffer, pH: 7.5.

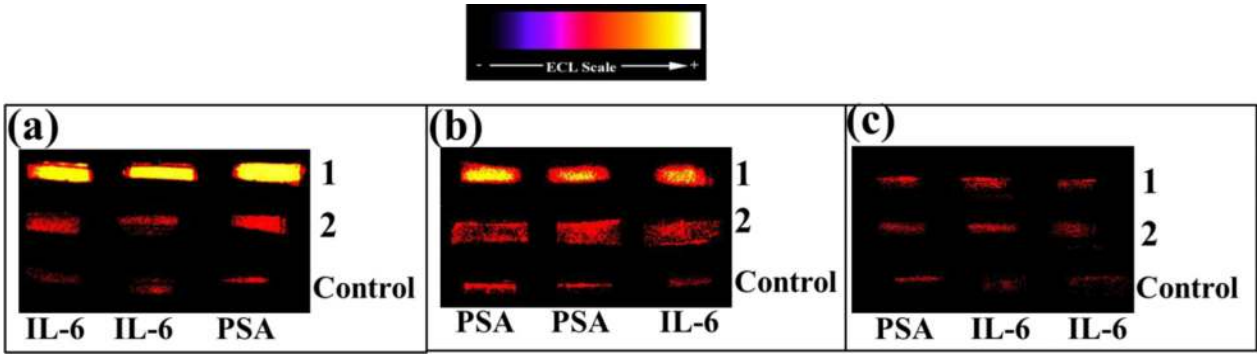

Fig. 3.

CCD images or microfluidic immunoarrays showing reproducibility for simultaneously detected PSA and IL-6 in calf serum on the same chip; (a) Lanes: **1**) 5 ng mL^{-1} PSA and **2**) 20 pg mL^{-1} IL-6, (b) Lanes: **1**) 100 pg mL^{-1} PSA and **2**) 200 pg mL^{-1} IL-6, and (c) Lanes: **1**) 100 fg mL^{-1} PSA and **2**) 10 fg mL^{-1} IL-6. In all images, controls are 0 pg mL^{-1} IL-6 and 0 pg mL^{-1} PSA. ECL image obtained at 0.95 V vs. Ag/AgCl in the presence of 0.05% Tween 20 + 0.05% Triton-X 100 + 100 mM TPrA in 0.2 M phosphate buffer, pH 7.5.

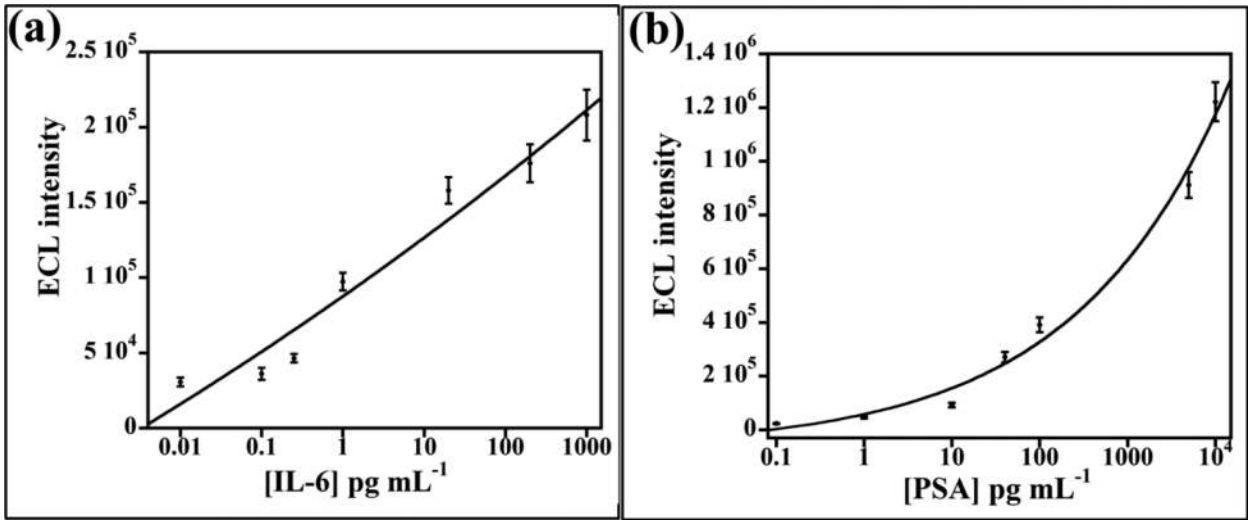

Fig. 4.

Calibration of array responses accumulated for 400 s for PSA and IL-6 mixtures in calf serum: (a) influence of IL-6 concentration on ECL signal and (b) influence of PSA concentration on ECL signal. ECL intensity for each antigen was plotted after subtracting relative ECL for protein-free controls. Error bars show standard deviations (n = 3).

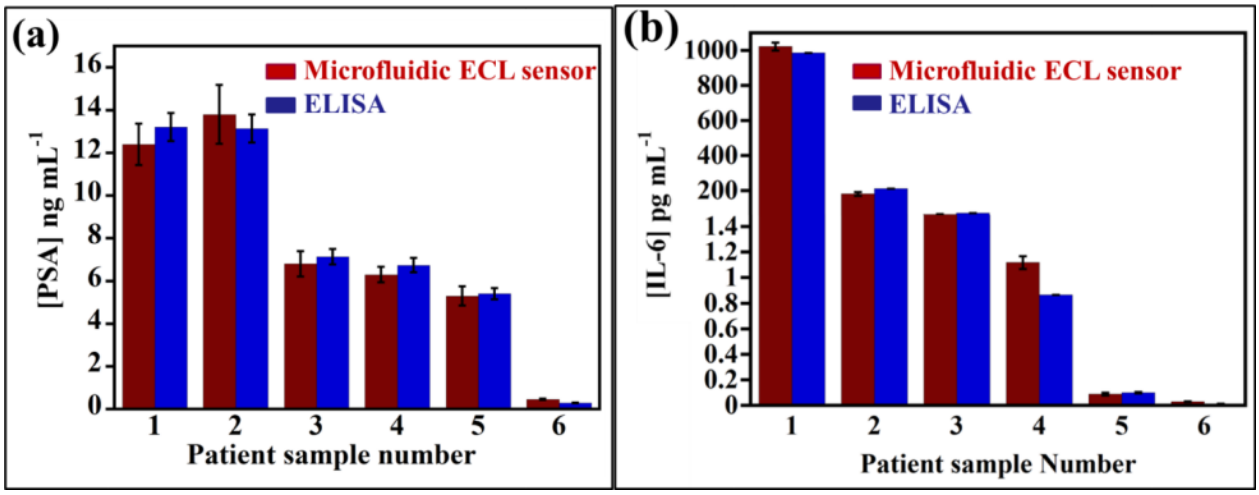

Fig. 5.

Comparison of microfluidic immunoarray determinations of PSA and IL-6 in synthetic pooled serum samples with individual single-protein ELISAs on the same samples. Error bars show standard deviations (n = 3). Serum samples 1-5 represent cancer patients and sample 6 a cancer cancer-free patients. (a) PSA detection (b) IL-6 detection, serum samples spiked with [IL-6]; sample 1 (1 ng mL^{-1}), sample 2 (200 pg mL^{-1}), sample 3 (20 pg mL^{-1}), sample 4 (1 pg mL^{-1}) sample 5 (100 fg mL^{-1}), and sample 6 (10 fg mL^{-1}).

Table 1

ECL intensities and relative standard deviations for detection of different concentrations PSA and IL-6 in calf serum.

[PSA] pg mL^{-1}	ECL intensity	Relative standard deviation	[IL-6] pg mL^{-1}	ECL intensity	Relative standard deviation
0.1	23685	7.6	0.01	30627	9.8
1	46445	10	0.1	36174	10
10	270640	3.3	0.5	46454	6.1
40	409760	4.8	1	97346	6.1
100	556600	5.0	20	158000	5.5
5000	912020	5.3	200	176000	7.1
10000	1222000	6.0	1000	208000	8.1